Software Environment for Performance Simulation of Three-hop Wireless Relay Channels under the Influence of Rician Fading

Dragana Krstic
University of Niš,
Faculty of Electronic Engineering
Niš, Serbia
e-mail: dragana.krstic@elfak.ni.ac.rs

Petar Nikolic
TigarTyres
Pirot, Serbia
e-mail: nikpetar@gmail.com

Nenad Petrovic
University of Niš,
Faculty of Electronic Engineering
Niš, Serbia
e-mail: nenad.petrovic@elfak.ni.ac.rs

Zoran Popovic
Higher Technical School of Professional Studies,
Zvecan, Serbia
e-mail: z.popovix@live.com

Sinisa Minic
Faculty of Teacher Education in Prizren – Leposavic,
University of Pristina- Kosovska Mitrovica,
Serbia
e-mail: sinisa.minic@pr.ac.rs

***Abstract*— In this work, a three-hop wireless relay channels under the influence of Rician fading will be observed. Three-hop wireless relay system model is made as the product of three independent, but not necessarily identically distributed, Rician random variables. Some important wireless relay system performance of the first and second order, as cumulative distribution function, outage probability, level crossing rate and average fade duration will be determined and graphically presented. The impact of fading parameters will be highlighted based on presented graphs. Then, simulation software environment for modelling and planning the wireless three-hop relay systems performance under the influence of Rician fading will be described. The goal of this method is to minimize the transmission costs and provide the best possible Quality of Service for defined wireless transmission scenario.**

Keywords- Graphics Processing Unit (GPU); linear optimization; random variables; Rician fading; system performance, three-hop relaying system.

I. INTRODUCTION

Performance of three-hop wireless relay channels under the influence of fading have not yet been analyzed enough in available literature [1] - [5]. Different authors mainly analyze multi-hop relay systems with the application on dual-hop channels [6] - [8].

The multi-hop communication in relay systems is introduced for improving the quality of transmission in cellular and ad hoc networks because of transmit power limitations. The benefits of multi-hop relays are visible in rural areas with small population and low level of traffic density.

Multi-hop routing is the way of communication in radio networks where network coverage area is larger than radio range of single nodes [9]. So, to get to a destination, node can utilize other nodes as relays. This is also very justified for energy efficiency reasons. After the transceiver is the major source of power consumption in a node, and transmission to long distance needs high power, in many cases multi-hop routing is more energy efficient than single-hop transmission [10], [11]. Hence, relay technologies have the potential to offer extended cell coverage, better energy efficiency and improved capacity over the next generation wireless networks.

In wireless environments, properties of communications systems are disturbed notably due to the signal envelope fluctuations based of the presence of multipath fading [12] [13]. Because of that, it is of substantial importance to characterize these random fluctuations in terms of the fading characteristics and derive the first and second order system performance [14], [15].

Although the existence of a direct path between the transmitter and the receiver, called line of sight (LOS), is not a prerequisite for wireless communication, in many modern applications, with the reduction of the coverage area there is a LOS between the transmitter and receiver. The Rician distribution is used to mathematically describe these propagation conditions with LOS. This is the reason we use this fading model in our paper.

Namely, we consider here a three-hop relay channel, as a special case of multi-hop relay channel, under the presence of Rician fading. This case is important for the environment where an optical LOS is present. By our opinion, there are not enough reported papers in available literature on this topic.

This paper consists of seven sections. In introduction, the main terms are defined. The literature review is presented in the second section. In the third section, the system model is shown. The first order characteristics of the product of three Rician random variables (RVs) are defined in the fourth section, but the second order characteristics of this product are presented the fifth one. The graphs for all performance are plotted and parameters analysis is done. In the sixth section, software environment for smart city mobile network planning is introduced. The last section consists of concluding remarks.

II. Related Work

The closed-form expressions for the outage probability (Pout), the channel capacity (CC), and also the average symbol error probability (ASEP) were calculated in [6] for amplify-and-forward (AF) multi-hop relay network in the presence of Rayleigh fading. The analytical expressions are obtained for some scenarios of dual-hop relay systems.

The output signal from multi-hop relay system is product of random variables at hops outputs. In [16], multi-hop system in the presence of Nakagami fading is analyzed through N*Nakagami distribution as suitable for modeling of realistic wireless fading channels. Statistical analysis of cascaded Rician fading channels is given in [17]. Different performance is derived for both fading channels in terms of the Meijer G-function.

Our group of authors analyzed different products of RVs and obtained some system performance for dual and three-hop relay systems in closed forms in [3], [4], [18], [19]. Wireless dual-hop relay system in κ-μ short term fading environment is presented in [18]. An analytical approach for evaluating performance of dual-hop cooperative link over shadowed Ricean fading channels is shown in [19]. All performance of product of three Rayleigh RVs are presented in [3]. The product of three Nakagami-*m* RVs is observed in [4] and some statistical characteristics are derived.

Three-hop system is also observed in [2]. The second order characteristics for such three-hop relay system were derived. The knowing of second-order statistics (level crossing rate (LCR) and average fade duration (AFD)) of multipath fading channels help in better understanding the effects of fading and then easier mitigation. As example, the AFD determines the average length of error bursts in fading channels [20]. So, in fading channels with relatively large AFD, long data blocks will be significantly affected by the channel fades than short blocks [21].

A knowledge of this fact is necessary for better choose of the frame length for coded packetized systems, designing interleaved or non-interleaved concatenated coding methods [22], optimizing the interleaver size, choosing the buffer depth for adaptive modulation schemes [23] [24], throughput (efficiency) estimation of communication protocols, and so on. Empirically-verified formulas for the LCR and AFD of common multipath fading models are necessary for all observed applications.

III. System Model

The observed three-hop communication system is illustrated in Fig. 1 [7]. It consists of a source node, marked by (S), sending the information signal to the destination, marked by (D), using two consecutive relays, signed by R1 and R2.

All nodes are equipped with a single antenna operating in half-duplex mode. The contiguous relays help delivering the information to the destination. This is valid when the network nodes are under heavy shadowing, or when the distance between terminals is large, and also when the nodes suffer limited power resources [7].

IV. The First Order Performance of Product of Three Rician Random Variables

For description of three-hop wireless relay system it is necessary to derive the first-order characteristics of the product of three Rician RVs. In this context, PDF, CDF and Pout will be analyzed.

A. PDF of Product of Three Rician RVs

Rician fading is a stochastic model for radio propagation where the signal arrives at the receiver by several different paths when one of the paths, typically a line of sight signal or some strong reflection signals, is much stronger than the others.

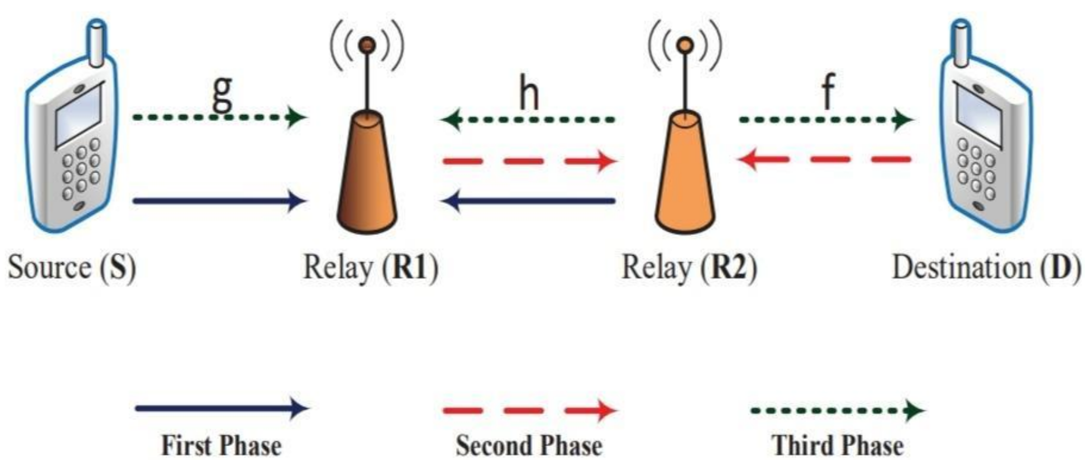

Figure 1. System model of a three-hop wireless relay [7].

In Rician fading, the amplitude gain is characterized by Rician distribution. It was named after Stephen O. Rice [25]. Rician RVs x_i have Rician distribution [25]:

$$p_{x_i}\left(x_i\right)=\frac{2\left(\kappa_i+1\right)}{\Omega_i e^{\kappa_i}}\sum_{j_i=0}^{\infty}\left(\frac{\left(\kappa_i+1\right)\kappa_i}{\Omega_i}\right)^{j_i}\frac{1}{\left(j_i!\right)^2}\cdot$$

$$\cdot\, x_i^{2j_i+1}e^{-\frac{\kappa_i+1}{\Omega_i}x_i^2},\ x_i\geq 0, \qquad (1)$$

where Ω_i are mean powers of RVs x_i, and κ_i are Rician factors. Rician factor is defined as a ratio of signal power of dominant component and power of scattered components. It can have values from [0, ∞].

A random variable x is product of three Rician RVs [3, eq. (2)]:

$$x=\prod_{i=1}^{3}x_i\ , \qquad (2)$$

which implies: $x_1=x/\,x_2\,x_3$.

Probability density function of product of three Rician RVs x is [26, eq. (7)]:

$$p_x\left(x\right)=\frac{2\left(\kappa_1+1\right)}{\Omega_1 e^{\kappa_1}}\sum_{j_1=0}^{\infty}\left(\frac{\left(\kappa_1+1\right)\kappa_1}{\Omega_1}\right)^{j_1}\frac{1}{\left(j_1!\right)^2}\cdot$$

$$\cdot\frac{2\left(\kappa_2+1\right)}{\Omega_2 e^{\kappa_2}}\sum_{j_2=0}^{\infty}\left(\frac{\left(\kappa_2+1\right)\kappa_2}{\Omega_2}\right)^{j_2}\frac{1}{\left(j_2!\right)^2}\cdot$$

$$\cdot\frac{2\left(\kappa_3+1\right)}{\Omega_3 e^{\kappa_3}}\sum_{j_1=0}^{\infty}\left(\frac{\left(\kappa_3+1\right)\kappa_3}{\Omega_3}\right)^{j_1}\frac{1}{\left(j_3!\right)^2}\cdot$$

$$\int_0^{\infty}dx_2\int_0^{\infty}dx_3 x_2^{-1-2j_1+2j_2}x_3^{-1-2j_1+2j_3}$$

$$\cdot\, x^{2j_1+1}e^{-\frac{\kappa_1+1}{\Omega_1}\left(\frac{x}{x_2x_3}\right)^2-\frac{\kappa_2+1}{\Omega_2}x_2^2-\frac{\kappa_3+1}{\Omega_3}x_3^2}. \qquad (3)$$

B. CDF of Product of Three Rician RVs

Cumulative distribution function (CDF) of product of three Rician RVs is [1]:

$$F_x\left(x\right)=\int_0^{\infty}dt\,p_x\left(t\right)=$$

$$=\frac{2\left(\kappa_1+1\right)}{\Omega_1 e^{\kappa_1}}\sum_{j_1=0}^{\infty}\left(\frac{\left(\kappa_1+1\right)\kappa_1}{\Omega_1}\right)^{j_1}\frac{1}{\left(j_1!\right)^2}\cdot$$

$$\cdot\frac{2\left(\kappa_2+1\right)}{\Omega_2 e^{\kappa_2}}\sum_{j_2=0}^{\infty}\left(\frac{\left(\kappa_2+1\right)\kappa_2}{\Omega_2}\right)^{j_2}\frac{1}{\left(j_2!\right)^2}\cdot$$

$$\cdot\frac{2\left(\kappa_3+1\right)}{\Omega_3 e^{\kappa_3}}\sum_{j_1=0}^{\infty}\left(\frac{\left(\kappa_3+1\right)\kappa_3}{\Omega_3}\right)^{j_1}\frac{1}{\left(j_3!\right)^2}\cdot$$

$$\int_0^{\infty}dx_2\int_0^{\infty}dx_3 x_2^{-1-2j_1+2j_2}x_3^{-1-2j_1+2j_3}e^{-\frac{\kappa_2+1}{\Omega_2}x_2^2-\frac{\kappa_3+1}{\Omega_3}x_3^2}$$

$$\int_0^{x}dt\,t^{2j_1+1}e^{-\frac{\kappa_1+1}{\Omega_1}\frac{t^2}{x_2^2x_3^2}}=$$

$$=\frac{2\left(\kappa_1+1\right)}{\Omega_1 e^{\kappa_1}}\sum_{j_1=0}^{\infty}\left(\frac{\left(\kappa_1+1\right)\kappa_1}{\Omega_1}\right)^{j_1}\frac{1}{\left(j_1!\right)^2}\cdot$$

$$\cdot\frac{2\left(\kappa_2+1\right)}{\Omega_2 e^{\kappa_2}}\sum_{j_2=0}^{\infty}\left(\frac{\left(\kappa_2+1\right)\kappa_2}{\Omega_2}\right)^{j_2}\frac{1}{\left(j_2!\right)^2}\cdot$$

$$\cdot\frac{2\left(\kappa_3+1\right)}{\Omega_3 e^{\kappa_3}}\sum_{j_1=0}^{\infty}\left(\frac{\left(\kappa_3+1\right)\kappa_3}{\Omega_3}\right)^{j_1}\frac{1}{\left(j_3!\right)^2}\cdot$$

$$\int_0^{\infty}dx_2\int_0^{\infty}dx_3 x_2^{-1-2j_1+2j_2+2j_1+2}x_3^{-1-2j_1+2j_3+2j_1+2}$$

$$\cdot\, e^{-\frac{\kappa_2+1}{\Omega_2}x_2^2-\frac{\kappa_3+1}{\Omega_3}x_3^2}$$

$$\cdot\frac{1}{2}\left(\frac{\Omega_1}{\kappa_1+1}\right)^{j_1+1}\gamma\left(j_1+1,\frac{\kappa_1+1}{\Omega_1}\frac{x^2}{x_2^2x_3^2}\right). \qquad (4)$$

In contrast to Rician, Rayleigh fading is a model for stochastic fading when there is no LOS signal. Since that it is considered as a special case of Rician fading. Rayleigh fading is obtained for Rician factor putting Rician factor κ=0. Because of that, derived expressions for CDF of product of three Rician RVs can be used for obtaining a CDF of product of three Rayleigh RVs, also for CDF of product of two Rayleigh RVs and Rician RV, and CDF of product of two Rician RVs and Rayleigh RV. The obtained results can be used in performance analysis of wireless three-hop relay radio system in the presence of multipath fading. This means that derived CDFs are used for the next cases: 1) when Rician fading is present in all three sections ($\kappa_i\neq 0$, i = 1, 2, 3), then 2) when Rayleigh fading is present in all three sections ($\kappa_1=\kappa_2=\kappa_3=0$), the next 3) when Rayleigh fading is present in two sections and Rician in one ($\kappa_1=\kappa_2=0$, $\kappa_3\neq 0$), and 4) when Rayleigh fading is present in one and Rician fading in two sections ($\kappa_1=0$, $\kappa_2\neq 0$, $\kappa_3\neq 0$). A case with $\kappa\rightarrow\infty$ presents the scenario without fading.

C. Outage probability of Product of Three Rician RVs

The outage probability is an important performance measure of quality of fading channels. Pout is defined as the probability that information rate is less than previously defined threshold information rate Γ_{th}. Actually, Pout is the probability that an outage occurs within a specified time period [14]:

$$P_{out} = \int_0^{\Gamma_{th}} p_x(t)dt, \tag{5}$$

where $p_x(x)$ is the PDF of the signal and Γ_{th} is the system protection ratio depending on the type of used modulation and the receivers' characteristics [27].

Using (4), Pout is expressed as [14]:

$$P_{out} = F_x(\Gamma_{th}). \tag{6}$$

Some graphs of the Pout are presented in Figs. 2 and 3 for different values of parameters.

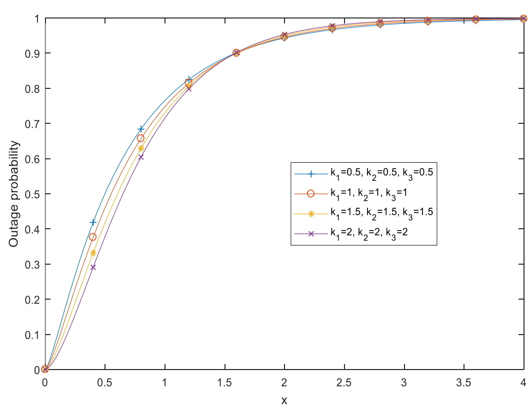

Figure 2. Outage probability of product of three Rician RVs versus signal envelope x for different values of Rician factor κ_I and signal power Ω=1.

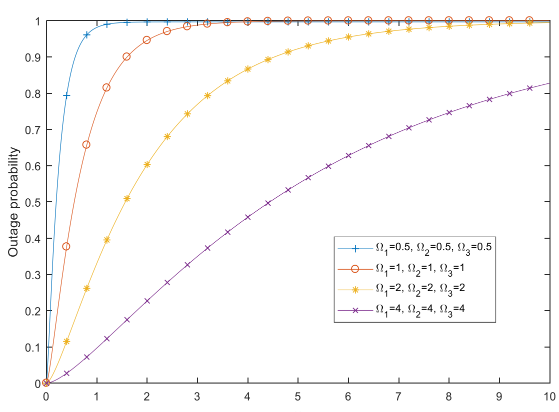

Figure 3. Outage probability of product of three Rician RVs depending on signal envelope for different values of signal power Ω_i and Rician factor κ=1.

The choice of parameters illustrates the broad range of shapes that the curves of the resulting distribution can have. It is evident that performance is improved with an increase in Rician factors κ_i. Also, higher values of fading powers Ω_i tend to reduce the Pout and improve system performance, as it is expected.

V. The Second Order Performance of the Product of Three Rician Random Variables

Level crossing rate and average fade duration of the signal envelope are very important second-order statistics of wireless channel. They enable useful information about the dynamic temporal behavior of multipath wireless fading channels.

A. LCR of Product of Three Rician RVs

Level crossing rate is one of the most important second-order performance measures of wireless communication system. LCR has application in modelling and designing of communication systems, but also in the design of error correcting codes, optimization of interleave size and throughput analysis.

LCR is defined as the expected rate at which a fading signal envelope crosses the given level in the downward direction, expressed in crossings per second [15]. The LCR of RV shows how often the envelope crosses a predetermined threshold x [28]. Let us first determine $p_{x\dot{x}}(x\dot{x})$ (the joint probability density function (JPDF) between x and $\dot{x}$), then apply the Rice's formula [25, Eq. (2.106)] to finally calculate the LCR [13]:

$$N_x = \int_0^{\infty} d\dot{x}\,\dot{x}\,p_{x\dot{x}}(x\dot{x}). \tag{7}$$

LCR of product of three Rician RVs is derived in [5, eq. (20)]:

$$N_x = \frac{1}{\sqrt{2\pi}}\pi f_m \frac{\Omega_1^{1/2}}{(\kappa_1+1)^{1/2}} \cdot \frac{2(\kappa_1+1)}{\Omega_1} \cdot \frac{2(\kappa_2+1)}{\Omega_2} \cdot \frac{2(\kappa_3+1)}{\Omega_3} \cdot$$
$$\cdot \sum_{i_1=0}^{\infty}\sum_{i_2=0}^{\infty}\sum_{i_3=0}^{\infty} \left(\frac{\kappa_1(\kappa_1+1)}{\Omega_1}\right)^{i_1} \frac{1}{(i_1!)^2} \left(\frac{\kappa_2(\kappa_2+1)}{\Omega_2}\right)^{i_2} \frac{1}{(i_2!)^2}$$
$$\cdot \left(\frac{\kappa_3(\kappa_3+1)}{\Omega_3}\right)^{i_3} \frac{1}{(i_3!)^2} x^{2i_1+1}$$
$$\cdot \int_0^{\infty} dx_2 \int_0^{\infty} dx_3 \left(1 + \frac{x^2}{x_2^4 x_3^2}\frac{\Omega_2}{\kappa_2+1}\frac{\kappa_1+1}{\Omega_1} + \frac{x^2}{x_2^2 x_3^4}\frac{\Omega_3}{\kappa_3+1}\frac{\kappa_1+1}{\Omega_1}\right)^{1/2} \cdot$$
$$\cdot x_2^{-2i_1-1+2i_2+1} x_3^{-2i_1-1+2i_3+1} e^{-\frac{\kappa_1+1}{\Omega_1}\frac{x^2}{x_2^2 x_3^2} - \frac{\kappa_2+1}{\Omega_2}x_2^2 - \frac{\kappa_3+1}{\Omega_3}x_3^2}. \tag{8}$$

Last integral can be solved by using Laplace approximation theorem for solution the two-fold integrals [29]. It was solved in [5, Eqs. (22) - (29)] in the form:

$$\int_0^\infty dx_2 \int_0^\infty dx_3 g\left(x_2, x_3\right) e^{\lambda f\left(x_2, x_3\right)} =$$

$$= \frac{\pi}{\lambda} g\left(x_{20}, x_{30}\right) e^{\lambda f\left(x_{20}, x_{30}\right)} \frac{1}{\left(B\left(x_{20}, x_{30}\right)\right)^{1/2}}. \qquad (9)$$

Some graphs for normalized LCR of product of three Rician RVs versus this product x are plotted in Figs. 4 and 5 [1] for different values of Rician factor κ_i and average power Ω_i.

It is visible that LCR increases when Rician signal power increases. The impact of signal envelope power on the LCR is higher for bigger values of Rician factor κ_i. Also, LCR increases with increasing of Ω_i for all values of signal envelope.

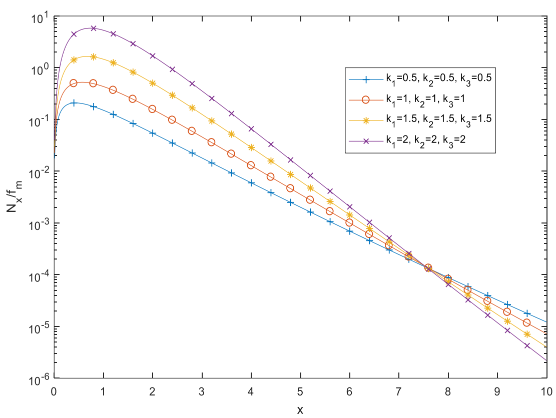

Figure 4. LCR normalized by f_m depending on signal envelope x for various values of Rician factor κ_i and signal power Ω=1.

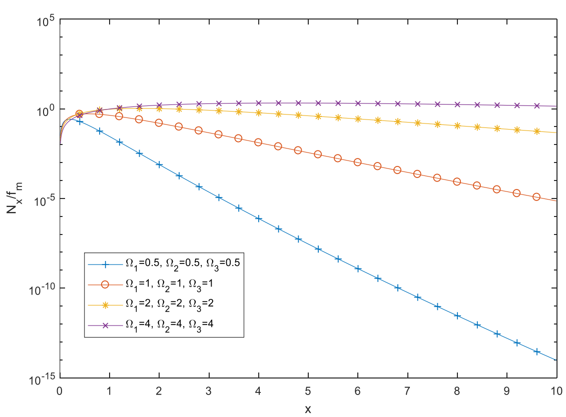

Figure 5. LCR normalized by f_m versus signal envelope x for various values of signal powers Ω_i.

The impact of signal envelope on the LCR is larger for higher values of the signal envelope, when Ω_i changes. It is known from theory that system has better performance for lower values of the LCR.

B. AFD of Product of Three Rician RVs

Average fade duration measures how long a signal's envelope or power stays below a given threshold, i.e., how long the user is in continuous outage. This is important for coding design.

AFD is derived from the LCR [4]. According to that, AFD is [30, eq. (9)]:

$$T_x(x) = \frac{P(x \le X)}{N_x(x)} = \frac{\int_0^X p_x(x) dx}{N_x(x)}. \qquad (10)$$

In numerator is actually the CDF of x from (4), and $N_x(x)$ is LCR given presented by (8) [31].

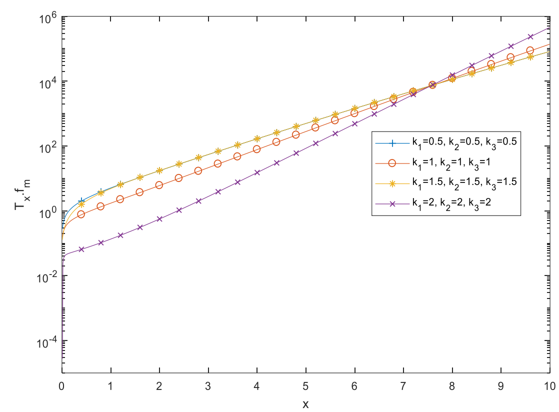

Figure 6. AFD normalized by f_m versus signal envelope x for different values of Rician factor κ_i and signal powers Ω_i=1.

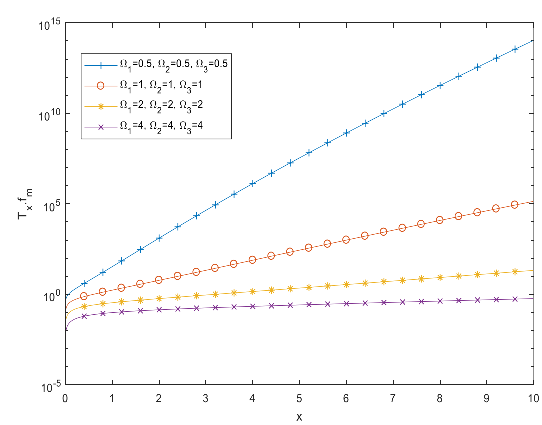

Figure 7. AFD normalized by f_m depending on signal envelope x for κ=1 and different values of signal powers Ω_i.

The normalized AFD ($T_x f_m$) of product of three Rician RVs is shown in Figs. 6 and 7 [1] depending on signal envelope x. One can observe from these figures that AFD has smaller values for higher parameter κ_i and lower signal envelope x. Also, it is possible to see from Fig. 7 that AFD increases for whole range of envelopes and lower Ω_i. The impact of Ω_i is bigger at higher envelopes' values.

VI. Software Environment for Smart City Mobile Network Planning

Moreover, we make use of the previously derived expressions within software simulation environment that aims optimal mobile network planning in order to support state-of-the-art services within smart cities. The tools are accessible using web browser and build upon the software engine presented in [8], [32], [33]. In Fig. 8, the workflow of this software environment is depicted.

The first step in this workflow represents creation of user-drawn smart city mobile network model relying on 3D graphical environment implemented using Three.js. When it comes to modelling, the following factors are taken into account: network provider's infrastructure (represented as base stations); terrain configuration (represented as different forms of obstacles, such as buildings and trees); end-users of provided network service (represented as autonomous cars, drones, surveillance cameras); smart city locations of interest, referred to as places.

Once user completes a network model, fading effect-related values are calculated: P_{out}, LCR and AFD relying on NVIDIA CUDA [34] which makes use of Graphics Processing Unit (GPU). This approach is beneficial, as the time required for these calculations is reduced due to impact of loop-level parallelization. Considering the fact that loop-based calculations represent the constituent part of fading expressions [35], significant acceleration was noticed in comparison with equivalent program written in Mathematica and executed entirely on CPU – 59 times for P_{out}, 61 times for LCR and 69 times for AFD. The structure generalized structure of CUDA C kernel is illustrated in Fig. 9, where *FadingMeasure* is changed with one of the fading-related measures – either P_{out}, LCR or AFD.

On the other side, we also make use of GPU hardware for prediction of service demand regarding the number of service consumers at given place within smart city. This prediction problem is treated as regression.

The input (independent) variables are the following: place id, day of the week, daily average temperature and daily number of COVID-19 cases, as each of them is assumed to be affecting how crowded certain place would be. The output is number of mobile network users. For this purpose, we use deep neural network with three hidden layers, 30 nodes per layer and ReLU activation function, while there is one linear node in the output layer.

Furthermore, Adam optimizer and Mean Squared Error cost function was used, with learning rate 0.01. The mean relative error of this model was around 6%. In Fig. 10, an excerpt of Python code relying on PyTorch [36] framework for deep learning, defining the proposed neural network is given. The approach to service demand prediction builds upon our previous work done in [37].

In the last step, once we have both the fading effect measures and service demand predictions calculated, the procedure of linear optimization can be executed in order to find the best possible selection of base stations, suitable for the selected smart city places. In this context, linear optimization model is written using AMPL 9 [38] and optimization problem solved relying on CPLEX [39] that implements simplex method.

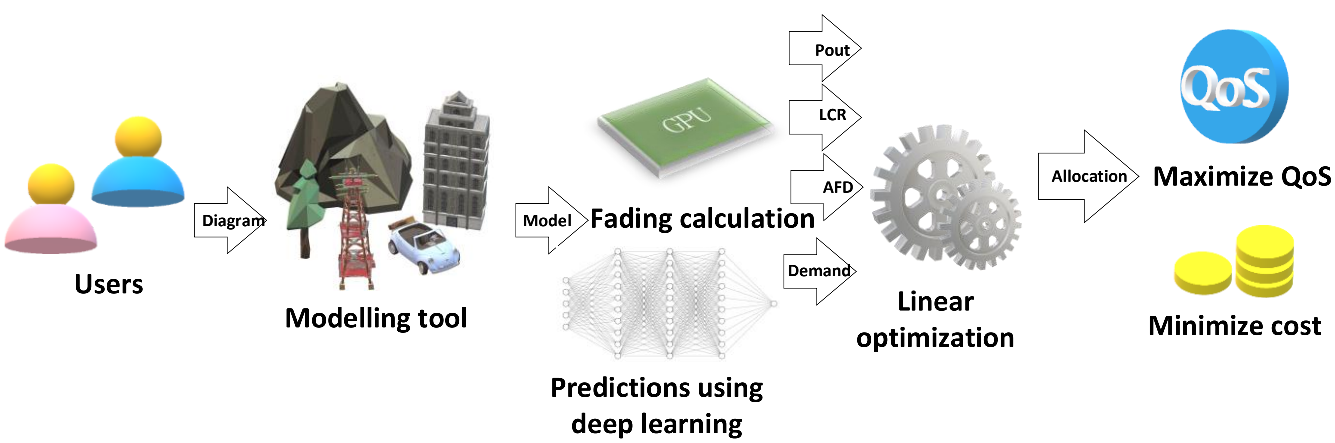

Figure 8. Smart city mobile network planning workflow.

```
__global__ void fading_kernel(Place* p, BStation* bs, float* fading)
{
    int k = threadIdx.x + blockIdx.x * blockDim.x;
    while (k < N)
    {
        out[k] = FadingMeasure(bs, p[k]);
        k += blockDim.x * gridDim.x;
    }
}
```

Figure 9. Generalized CUDA C kernel illustrating GPU-enabled fading effect calcualtion.

```
class ServiceDemandModel(torch.nn.Module):
    def __init__(self, input_length):
        super(ServiceDemandModel, self).__init__()
        self.input_num = input_num

        self.layer1 = torch.nn.Linear(input_length, 35)
        self.layer2 = torch.nn.Linear(35, 35)
        self.layer3 = torch.nn.Linear(35, 35)
        self.layer4 = torch.nn.Linear(35, 1)

    def forward(self, x):
        output = F.relu(self.layer1(x))
        output = F.relu(self.layer2(output))
        output = F.relu(self.layer3(output))
        nu = self.layer4(output)
        return nu

predictor=ServiceDemandModel(4)
```

Figure 10. Excerpt from Python code showing deep neural network definition using PyTorch for service demand prediction treated as regression.

In this case, the optimization model's objective function has goal to minimize the overall mobile network maintenance costs *dmc[bs, p]* for placing base station *bs* at place *p*. On the other side, it aims to maximize the network performance by keeping P_{out} and AFD as low as possible:

$$minimize \sum_{bs \in BS,\, p \in P} AFD[p,bs]Pout[p,bs]dmc[p,bs]x[p,bs] \cdot \tag{11}$$

Table I

Results for varying network model size.

Base stations [num]	Places [num]	P_{out} [s]	LCR [s]	AFD [s]	Pred [s]	Opt. [min]	Cost red. [%]
3	2	0.61	0.72	0.94	0.33	0.29	36
5	3	0.94	1.07	1.21	0.36	0.73	42
9	4	1.33	1.69	1.88	0.41	1.04	78
12	5	1.92	2.13	2.76	0.47	3.04	61

In this equation, *x[p, bs]* is decision variable that will take value 1 in case when base station *bs* is about to be allocated to place *p*, while it is 0 otherwise. Moreover, for each place p, the channel capacity [40] of a base station *cap[p, bs]* should be enough to handle the predicted number of users *nu[p]*:

$$\sum_{bs \in BS} x[p,bs]cap[p,bs] \geq nu[p],\; p \in P \cdot \tag{12}$$

Finally, when it comes to evaluation of the proposed approach making use the synergy of GPGPU calculations, deep learning and linear optimization, the cost reduction percentage and execution times for different sizes of network models (number of base stations and places) are presented in Table I. According to these results, it can be seen that it takes more processing time for larger models, while the cost reduction depends on the specific model instance.

VII. CONCLUSION

In this paper, we analyzed the influence of Rician fading to the three-hop wireless relay system. The output signal from such system was obtained as the product of three Rician RVs. For this scenario, we presented previously determined formulas for the next performance: PDF, CDF, Pout, LCR and AFD. Based on the presented results it is possible to anticipate the behavior of the real wireless relay system in the presence of Rician fading. The parameters influence is analyzed based on plotted graphics.

Finally, in the last part of this paper, the previously derived expressions for performance of wireless system in the presence of fading were incorporated into GPU-enabled network planning environment. Considering the achieved results, it can also be concluded that the proposed approach leveraging synergy of GPGPU calculations, deep learning and linear optimization, enables more efficient network planning. This approach provides the highest possible Quality of Service (QoS), keeping at the same time the costs as lowest as possible. The procedure depends also on the specific fading conditions in smart city.

ACKNOWLEDGMENT

This article was realized under the projects of the Ministry of Education, Science and Technological Development of the Republic of Serbia.

REFERENCES

[1] D. Krstic, P. Nikolic, S. Minic, and Z. Popovic, "Some Performance of Three-hop Wireless Relay Channels in the Presence of Rician Fading", The Sixteenth International Conference on Wireless and Mobile Communications ICWMC 2020, October 18, 2020 to October 22, 2020 - Porto, Portugal, pp. 18-23.

[2] D.-H. Kim, Y.-C. Ko, and S. Park, "Three-hop MIMO relaying systems in Gaussian broadcast channels", 2nd International Conference on Signal Processing and Communication Systems, ICSPCS, Australia, Gold

Coast, 15-17 December 2008. doi:10.1109/icspcs.2008.4813661

[3] D. Krstic, P. Nikolic, Z. Popovic, and M. Stefanovic, “First and second order characteristics of wireless three-hop relay channel with presence of Rayleigh fading”, Journal of Telecommunications and Information Technology (JTIT), no. 2/2020, pp. 36-44, https://doi.org/10.26636/jtit.2019.130018

[4] D. Krstic, P. Nikolic, I. Vulic, S. Minic, and M.Stefanovic, “Performance of the product of three Nakagami-m random variables”, Journal of Communications Software and Systems (JCOMSS), vol. 16, no. 2, June 2020, pp. 122-130, http://dx.doi.org/10.24138/jcomss.v16i2.989

[5] D. Krstic, M. Stefanovic, M.M.B. Yaseen, S.Aljawarneh, and P. Nikolić, „Statistics of the product of three Rician random processes with application”, International Conference on Data Science, E-learning and Information Systems 2018 (Data'18), Madrid, Spain, October 1-2, 2018. DOI: 10.1145/3279996.3280015

[6] A. Panajotovic, N. Sekulovic, A. Cvetkovic, and D.Milovic, “System performance analysis of cooperative multihop relaying network applying approximation to dual-hop relaying network”, Int. J. Commun Syst. 2020; e4476, p. 1-10, https://doi.org/10.1002/dac.4476

[7] A. Kuhestani, M. T. Mamaghani, and H. Behroozi, “A new secure multi-hop untrusted relaying scheme“, ArXiv, Corpus ID: 162184290, May 2019.

[8] D. Milić, S. Suljović, N. Petrović, S. Koničanin, and S.Panić, “Software environment for performance of relay signal by DF technique influenced by k-μ fading”, INFOTEH 2020, pp. 1-4, 2020. https://doi.org/10.1109/INFOTEH48170.2020.9066304

[9] N. Athanasopoulos, P. Tsiakas, K. Voudouris, I. Georgas, and I. Agapiou, Multi-hop Relay in Next Generation Wireless Broadband Access Networks: An Overview. In: Chatzimisios P., Verikoukis C., Santamaría I., Laddomada M., Hoffmann O. (eds) Mobile Lightweight Wireless Systems. Mobilight 2010. Lecture Notes of the Institute for Computer Sciences, Social Informatics and Telecommunications Engineering, vol 45. Springer, Berlin, Heidelberg, 2010. https://doi.org/10.1007/978-3-642-16644-0_47

[10] U. M. Pešović, J. J. Mohorko, K. Benkič, and Ž. F. Čučej, “Single-hop vs. Multi-hop – Energy efficiency analysis in wireless sensor networks”, Telekomunication forum TELFOR, Serbia, Belgrade 23–25 November 2010, pp. 471–474.

[11] S. Fedor and M. Collier, “On the problem of energy efficiency of multi-hop vs one-hop routing in Wireless Sensor Networks”, 21st International Conference on Advanced Information Networking and Applications Workshops (AINAW'07)

[12] P. M. Shankar, Fading and shadowing in wireless systems, Springer, New York Dordrecht Heidelberg London. 2012, DOI 10.1007/978-1-4614-0367-8.

[13] G. L. Stüber, Principles of Mobile Communications, 2nd ed., MA, USA, Springer, 2001. ISBN 978-1-4614-0364-7

[14] M. K. Simon and M. S. Alouini, Digital communication over fading channels, (2nd ed.). New York, Wiley-IEEE Press. ISBN: 978-0-471-64953-3, 2004.

[15] A. Goldsmith, Wireless Communications, Cambridge University Press, 2005, DOI: https://doi.org/10.1017/CBO9780511841224

[16] G. K. Karagiannidis, N. C. Sagias, and T. Mathiopoulos, “The N*Nakagami fading channel model”, 2005 2nd International Symposium on Wireless Communication Systems, Siena, Italy, 5-7 Sept. 2005, pp. 185-189, DOI: 10.1109/ISWCS.2005.1547683

[17] I. Ghareeb and D. Tashman, “Statistical analysis of cascaded Rician fading channels”, International Journal of Electronics Letters, November 2018. doi:10.1080/21681724.2018.1545925

[18] D. Krstic, M. Stefanovic, R. Gerov, and Z. Popovic, “Wireless relay system with two sections in κ-μ short term fading channel”, The Twelfth Iinternational Conference on Wireless and Mobile Communications, ICWMC 2016, Barcelona, Spain, Nov. 13 - 17, 2016, pp. 110 - 114.

[19] A. Cvetković, J. Anastasov, S. Panić, M. Stefanović, and D. Milić,.”Performance of dual-hop relaying over shadowed Ricean fading channels”, Journal of Electrical Engineering, 2011, 62(4), pp. 244–248. doi:10.2478/v10187-011-0039-6

[20] C. Wang and D. Xu, “A study on burst error statistics and error modelling for MB-OFDM UWB systems”, IET Seminar on Ultra Wideband Systems, Technologies and Applications, 2006, p. 244-248, DOI: 10.1049/ic:20060518

[21] A. Abdi, K. Wills, H. A. Barger, M.-S. Alouini, and M.Kaveh, “Comparison of the level crossing rate and average fade duration of Rayleigh, Rice, and Nakagami fading models with mobile channel”, 52nd Vehicular Technology Conference IEEE VTS Fall VTC2000, Boston, MA, USA, pp. 1850-1857, DOI: 10.1109/VETECF.2000.886139

[22] J. M. Morris and J. L. Chang, “Burst error statistics of simulated Viterbi decoded BFSK and high-rate punctured codes on fading and scintillating channels,” IEEE Trans. Commun., vol. 43, pp. 695-700, 1995.

[23] A. J. Goldsmith and S. G. Chua, “Variable-rate coded M-QAM for fading channels", IEEE Trans. Commun., vol. 45, pp. 1218-1230, 1997.

[24] G. N. Onoh, T. L. Alumona, and C. O. Ezeagwu, “Adaptive modulation techniques for capacity improvement of BER in WCDMA”, International Journal of Advanced Research in Computer Engineering & Technology (IJARCET), Vol. 4, Issue 9, September 2015, pp. 3537-3542.

[25] S. O. Rice, “Mathematical analysis of random noise”, Bell System Technical Journal, 23(3), 1944, pp. 282–332. doi:10.1002/j.1538-7305.1944.tb00874.x

[26] D. Krstic, P. Nikolic, Z. Popovic, S. Minic, and M.Stefanovic, ”Moments of signals over wireless relay fading environment with line-of-sight”, SoftCom 2020, Hvar, Croatia, September 17-19,2020.DOI: 10.23919/SoftCOM50211.2020.9238347

[27] I. Trigui, A. Laourine, S. Affes, and A. Stephenne, “Outage analysis of wireless systems over composite fading/shadowing channels with co-channel interference”, IEEE Wireless Communications and Networking Conference, 5-8 April 2009, Budapest, Hungary

[28] W. C. Jakes, Microwave Mobile Communications. Piscataway, NJ: IEEE Press, 1994.

[29] J. L. Lopez and P. J. Pagola, “A simplification of the laplace method for double integrals. Application to the second appell function”, Electronic Transactions on Numerical Analysis, vol. 30, 2008.

[30] T. T. Tjhung and C. C. Chai, “Fade statistics in Nakagami-lognormal channels”, IEEE Transactions on Communications, 1999, 47(12), pp. 1769–1772. doi:10.1109/26.809692

[31] X. Dong and N. C. Beaulieu, “Average level crossing rate and average fade duration of selection diversity”, IEEE Communications Letters, 5(10), 2001, pp. 396–398, doi:10.1109/4234.957373

[32] N. Petrović, S. Koničanin, D. Milić, S. Suljović, and S. Panić, "GPU-enabled framework for modelling, simulation and planning of mobile networks in smart sities", ZINC 2020, pp. 1-6, 2020, https://doi.org/10.1109/ZINC50678.2020.9161773

[33] N. Petrović, S. Vasić, D. Milić, S. Suljović, S. Koničanin, "GPU-Supported Simulation for ABEP and QoS analysis of a Combined Macro Diversity System in a Gamma-Shadowed k-µ fading channel", Facta Universitatis: Electronics and Energetics Vol. 34, No 1, March 2021, pp. 89-104. https://doi.org/10.2298/FUEE2101089P

[34] J. Sanders, E. Kandort, CUDA By Example: An Introduction to General-Purpose GPU Programming, Addison-Wesley, 2011.

[35] A. F. Abdelrazek, M. Kaschub, C. Blankenhorn, M. C. Necker, "A Novel Architecture using NVIDIA CUDA to speed up Simulation of Multi-Path Fast Fading Channels", pp. 1-5, 2009.

[36] E. Stevens, L. Antiga, T. Viehmann, Deep Learning with PyTorch, Manning Publications, 2020.

[37] D. Krstić, S. Suljović, N. Petrović, S. Minić, "Effects of Weibull fading and co-channel interference shape and scale parameters and number of branches on multi-branch SC receiver outage performance", 15th International Online Conference on Applied Electromagnetics - ΠΕС 2021, pp. 141-144, 2021.

[38] R. Fourer, D. Gay, B. Kernighan, AMPL: A Modeling Language for Mathematical Programming, Duxbury Press, 2003.

[39] IBM CPLEX Optimizer [online]. Available on: https://www.ibm.com/analytics/cplex-optimizer, last accessed: 01/03/2021.

[40] D. Krstić, S. Suljović, N. Petrović, Z. Popović, S. Minić, "Channel Capacity of Macrodiversity System in Gamma Shadowed k-µ Fading Environment", AIIT 2020 International conference on Applied Internet and Information Technologies, pp. 125-130, 2020.